



A Schiff-base cross-linked supramolecular polymer containing diiminophenol compartments and its interaction with copper(II) ions

Marcel Klein-Hitpaß, Amy D. Lynes, Chris S. Hawes, Kevin Byrne, Wolfgang Schmitt & Thorfinnur Gunnlaugsson


To cite this article: Marcel Klein-Hitpaß, Amy D. Lynes, Chris S. Hawes, Kevin Byrne, Wolfgang Schmitt & Thorfinnur Gunnlaugsson (2017): A Schiff-base cross-linked supramolecular polymer containing diiminophenol compartments and its interaction with copper(II) ions, *Supramolecular Chemistry*, DOI: [10.1080/10610278.2017.1362108](https://doi.org/10.1080/10610278.2017.1362108)

To link to this article: <http://dx.doi.org/10.1080/10610278.2017.1362108>

 View supplementary material 

 Published online: 08 Aug 2017.

 Submit your article to this journal 

 View related articles 

 View Crossmark data 



A Schiff-base cross-linked supramolecular polymer containing diiminophenol compartments and its interaction with copper(II) ions

Marcel Klein-Hitpaß,^{a,b} Amy D. Lynes,^a Chris S. Hawes,^a Kevin Byrne,^c Wolfgang Schmitt^c and Thorfinnur Gunnlaugsson^a

^aSchool of Chemistry and Trinity Biomedical Sciences Institute (TBSI), University of Dublin, Trinity College Dublin, Dublin 2, Ireland; ^bOrganic Chemistry Institute and Center for Soft Nanoscience, Westfälische Wilhelms-Universität Münster, Münster, Germany; ^cSchool of Chemistry and Centre for Research on Adaptive Nanostructures and Nanodevices, Trinity College Dublin, Dublin 2, Ireland

ABSTRACT

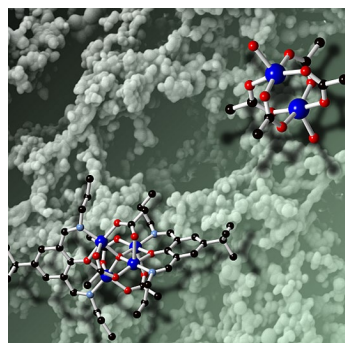
We report here the preparation of a Schiff-base linked organic polymer **1** based on linkages containing the potent supramolecular aggregator benzene-1,3,5-tricarboxamide, connected through 2,6-diiminophenol metal binding pockets into a cross-linked polymer. The morphological and physical properties of this material are studied using electron microscopy techniques, thermal analysis, NMR, fluorescence spectroscopy and gas adsorption studies. The interaction of the polymer **1** with Cu^{II} ions is then investigated by soaking the material with methanolic copper acetate solution, and studying the resulting aggregates using EDX microscopy and FTIR spectroscopy. A small-molecule model compound **2** is also prepared and crystallographically characterised to act as a spectroscopic comparison, providing strong evidence that **1** interacts with copper ions through a nucleation/seeding mechanism for the growth of microcrystalline copper acetate deposits, rather than via chemisorption of the copper ions within the diiminophenol binding pockets. Preliminary results suggest a similar mechanism for Co^{II} adsorption, while Zn^{II} ions exhibit a separate interaction mode.

ARTICLE HISTORY

Received 10 May 2017
Accepted 23 July 2017

KEYWORDS

Supramolecular chemistry; organic polymers; Schiff base; self-assembly; benzene-1,3,5-tricarboxamide




1. Introduction

The formation of supramolecular soft materials, for example gels and polymers, has become a widely studied area in recent years, with much current interest in the assembly pathways and the influence of chemical constituents on the bulk properties of such materials (1). The rational design of these systems based on well-established modes of intermolecular interaction, aggregation properties, host-guest recognition behaviour and directed

self-assembly properties have already led to many fruitful advances towards functional materials (2). Applications of such soft matter include, but are not limited to, drug delivery agents, crystal growth media and organocatalysts (3). Of particular interest to our group and others is the study of soft materials and supramolecular polymers based on a central benzene-1,3,5-tricarboxamide (BTA) core (4). Combining their simple structure and the ease of varying their functionality with an already detailed

CONTACT Thorfinnur Gunnlaugsson  gunnlaut@tcd.ie

 Supplemental data for this article can be accessed at <https://doi.org/10.1080/10610278.2017.1362108>.

© 2017 Informa UK Limited, trading as Taylor & Francis Group

understanding of their supramolecular self-assembly behaviour, a number of uses based on this material have been reported ranging from, for example, biomedical applications to nanotechnology (5). BTA offers a readily modifiable core, often giving materials which retain the key triple-stranded helical hydrogen-bonding aggregation mode, and acting as an ideal family of compounds for systematic studies (6). It has been widely reported that the bulk properties of the resulting materials can be modulated by chemically altering the nature of the side chains attached to the BTA core (7). In particular, it has also been reported that metal coordination can further influence the nature of the materials formed, and impart specific metal-centred functionalities to the resulting materials (8).

As a powerful synthon in self-assembled supramolecular systems, the Schiff base linkage has been put to use in the synthesis of a wide variety of intricate molecular architectures (9). As well as being widely used in discrete systems, including helicates and metal-organic polyhedra (10), and in the development of organic 'dynamic combinatorial' systems (11), the Schiff base linkage has been successfully employed as a linking element in the formation of covalent organic polymers and related extended organic systems (12). The metal binding affinity of Schiff base groups is well established, often utilised in metal-templated syntheses, and is exemplified by the Robson macrocycle and related oligo-iminophenolate compounds obtained from the reaction of polyamines with 2,6-diformylphenol and its analogues (13). The parent macrocycle, formed from the reaction between 4-methyl-2,6-diformylphenol and 1,3-propanediamine, is well established as a potent chelator for transition metal ions (14), and displays a great deal of synthetic versatility, leading to extensive studies into the molecular magnetism and catalytic properties of its various transition metal adducts and those of related, Schiff-base compartment ligands (15). Due to their well-established coordination chemistry and ready availability, 2,6-diiminophenol-derived synthons are prime candidates as linking groups for functional organic polymers (16), readily assembling in solution and containing the capacity for potential metal chelation. Herein, we detail our attempts to realise a functional Schiff base-containing organic polymer using a combined BTA/diiminophenol linking strategy, and describe the physical and morphological properties of the resulting material and its interaction with Cu^{II} ions with the aid of a small-molecule spectroscopic model compound. The result is a hybrid supramolecular system incorporating structural features that can potentially participate in classical supramolecular interactions including hydrogen bonding, π - π interactions and metal coordination.

2. Results and discussion

2.1. Synthesis, structure and properties of polymer 1

With the aim of preparing an organic polymer containing aggregation-inducing BTA groups and Schiff base metal-binding compartments, a reversible imine, or Schiff base, condensation between an amino-substituted BTA derivative and a 2,6-diformylphenol derivative was conceived. The reaction of trimethyl-1,3,5-benzenetricarboxylate with ethylenediamine, based on an established procedure by Xu et al. (17) and outlined in Scheme 1, yielded the triamine building block *N,N',N''*-tris(2-aminoethyl)-1,3,5-benzenetricarboxamide in near-quantitative yield. Previously, we have reported alkylamine-substituted BTA derivatives which exhibit interesting morphological properties related to their tendency towards aggregation in solution and gel phases (2b, 4b–c). As such, we investigated the morphological properties of the triamine compound *N,N',N''*-tris(2-aminoethyl)-1,3,5-benzenetricarboxamide by drop-casting suspensions or solutions of the compound in ethanol, ethanol/TFA and ethanol/NH₄OH. Despite our expectations, however, no morphological features consistent with extended fibrous aggregation were observed on this length scale (Supporting Information).

To allow for the formation of an organic polymer through reversible bond formation, the triamine was then reacted with commercially available 4-*tert*-butyl-2,6-diformylphenol at room temperature in ethanol, yielding polymer **1** as a yellow solid. The polymer was insoluble in common solvents, necessitating analysis purely by solid-state methods. The solid-state ¹³C {CP-MAS} NMR spectrum was collected, and compared to the solution-state spectra of the starting materials (Supporting Information). The carbonyl signal of the dialdehyde precursor (193 ppm) disappears in the spectrum of **1**, being replaced by an imine resonance, which overlapped with the amide and *ipso*-phenol signals in the 150–175 ppm region. The signal at ~60 ppm is consistent with the CH₂ group nearest the imine nitrogen atom, which exhibits a downfield shift following the Schiff base formation. X-ray powder diffraction (Supporting Information) revealed that the material is essentially amorphous in nature. This solid also exhibited a broad fluorescence emission band upon excitation at 366 nm or 430 nm, with the emission maxima occurring in both cases at 560 nm. In comparison, the solid-state emission spectrum of the aldehyde precursor exhibited a significantly narrower emission band, with the emission maximum blue-shifted to 540 nm when irradiated under equivalent conditions (Figure 1). These variations are further indicative of the chemical transformation undergone by the phenolic fluorophore. The FTIR analysis of this polymer will be discussed below.

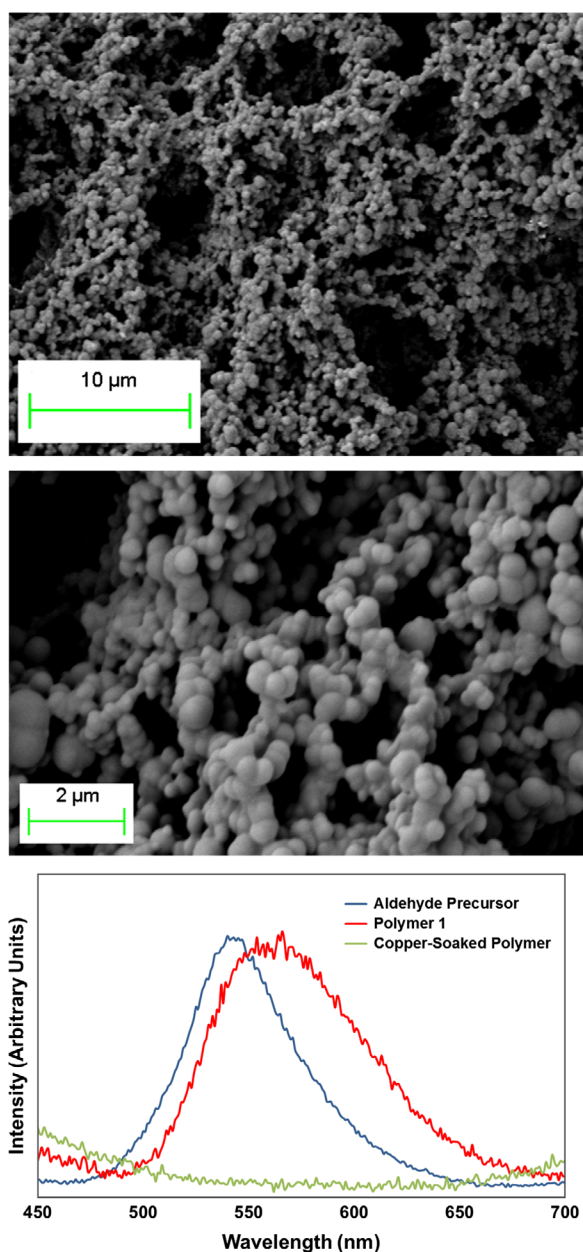


Figure 1. (Colour online) (Top/Middle) Scanning electron microscopy (SEM) images of polymer **1** grown directly onto a silicon support; (Bottom) Emission spectra ($\lambda_{\text{ex}} = 366 \text{ nm}$) for polymer **1** (red), the precursor aldehyde (blue) and the copper-soaked polymer **1**-Cu (green) in the solid state.

Thermogravimetric analysis (TGA) was also carried out on polymer **1** (Supporting Information). The curve indicates the presence of encapsulated volatile species, most likely solvent molecules, consistent with the results of elemental analysis that indicated encapsulated water (most likely either retained after drying *in vacuo* at room temperature or re-adsorbed from exposure to air). A steep loss of mass occurs in the range 25–50 °C, followed by a gradual loss in mass continuing until approximately 300 °C. This is followed by a multi-step decomposition process

initiating at 325 °C, again followed by a gradual mass loss up to 500 °C. The morphology of **1** was analysed by Scanning Electron Microscopy (SEM), with the polymer deposited onto the silicon surface itself by carrying out the condensation reaction with the silicon slide immersed in the reaction medium, and the sample dried *in vacuo* before SEM analysis. The images obtained, Figure 1, reveal a tightly packed polymer network, with the individual particles having a smooth, approximately spherical shape. The spherical particles appear smoothly fused to one another, forming a thick layer on the silicon support. Analysis of a sample of **1** by N_2 adsorption at 77 K reveals a low-capacity type II isotherm, with relatively low BET surface area of ca. 12 m^2/g (Supporting Information), suggesting a broad distribution of pore sizes and no significant microporosity within the material.

Following the preparation and characterisation of **1**, the interaction between the polymer and copper(II) ions in solution was investigated. Immersion of **1** into a solution of copper acetate hydrate in methanol (5 mg/mL) caused a darkening in colour of the material from yellow to dark green/brown (Figure 2). Attempts to quantify this adsorption process by UV-Visible absorption analysis of the supernatant solution showed no appreciable decrease in copper concentration of the supernatant after 22 h of immersion, implying the total capacity for copper uptake was sub-stoichiometric. SEM analysis of polymer **1** after soaking in 5 mg/mL copper acetate solution for 24 h revealed the original morphology of the polymer was maintained, but small crystallites were present on the surface of the particles as shown in Figure 2. The nature of the surface coating and the extent of coverage of the particle surface was further probed using Energy-Dispersive X-ray Spectroscopy (EDX). EDX was carried out on both the polymer **1** alone and on the copper soaked polymer, and revealed the presence of copper on the surface of the soaked polymer, while the original polymer was purely organic in nature (Supporting Information). A line mapping EDX experiment showed that the copper species was dispersed co-incident with the organic material and separate from any potential superficial copper coating artefacts present on the silicon support (Figure 2). Although exhibiting a crystalline appearance by SEM, the copper-containing coating was not present in sufficient quantities to be detectable by X-ray powder diffraction in the presence of the large amorphous background from the polymer itself (Supporting Information), an observation also consistent with a low surface loading of copper within the material. Nonetheless, soaking polymer **1** in copper caused complete loss of the fluorescence emission band of the pristine polymer (Figure 1); this is most likely either due to absorption from the surface layer at the excitation wavelength or

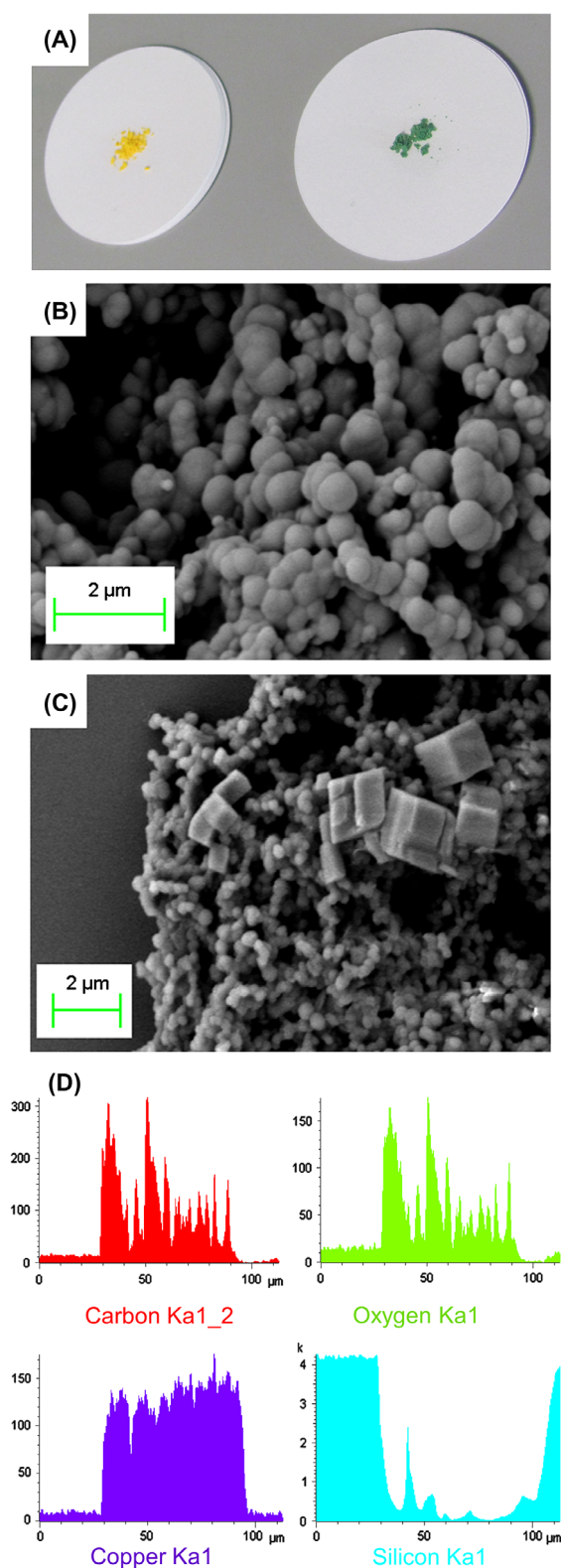


Figure 2. (Colour online) Results of copper soaking experiments on polymer **1**: (A) Photographs of the pristine yellow polymer **1** and green copper-soaked **1-Cu**; (B) SEM image of the polymer prior to contact with copper solution; (C) SEM image of **1** after immersion in copper acetate solution and drop-casting onto silicon support, showing the growth of crystallites; (D) EDX line mapping experiment on **1-Cu** showing intensity profiles for (clockwise from top left) C, O, Si and Cu K α bands.

through an electronic quenching mechanism originating from the d⁹ copper(II) ions present at the surface.

2.1.1. Synthesis and structure of model compound **2**

In order to gain a more quantitative understanding of the possible modes of interaction between copper ions and the polymer **1**, a model compound was prepared containing a single diiminophenol binding site with *n*-propyl tails, with the intention of combining X-ray structural data with FTIR evidence of the binding site and ultimately comparison with the copper-soaked polymer **1**. Ligand **HL** was prepared by the *in situ* reaction of 4-*tert*-butyl-2,6-diformylphenol with two equivalents of *n*-propylamine in methanol at reflux. Attempts to crystallise metal complexes of this ligand directly from the reaction mixture or from other alcohol solvents to mimic the soaking conditions for **1** were unsuccessful, and as such, acetonitrile was used as a surrogate. The yellow methanolic solution of **HL** was evaporated under reduced pressure to give a yellow oil, which was then taken up directly in acetonitrile and combined with an acetonitrile solution of Cu(II) acetate hydrate. Allowing the resulting green solution to stand for 48 h yielded dark green crystals in an overall yield of 9% based on the starting aldehyde, which were isolated by filtration and subjected to single-crystal X-ray diffraction.

The diffraction data for [Cu₄O(OAc)₄(L)₂] **2** were solved and the structural model refined in the monoclinic space group *P*2₁/*c*, with the asymmetric unit containing the molecule in its entirety and no associated solvent molecules or guests. The complex itself consists of a tetrahedral Cu₄O centre containing a μ₄-oxo core, surrounded by four μ₂-κO:κO' acetato ligands each bridging between two pairs of copper ions as shown in Figure 3. The remaining coordination sites are occupied by two molecules of **L**, each bridging two copper ions in a μ₂-κO,N:κO,N' coordination mode. Each copper ion adopts a semi-regular square pyramidal geometry with typically elongated axial Cu–O distances in the range 2.261(6)–2.396(6) Å, compared to equatorial Cu–O distances, which lie in the range 1.915(5)–2.007(5) Å. The six unique Cu–Cu distances fall in the range 3.0154(14)–3.1983(14) Å, and are typical for complexes with [Cu₄O] cores (18). The overall structure of complex **2** is closely related to similar materials derived from other 4-substituted 2,6-diformylphenols and various alkylamines under similar reaction conditions (19), and can be considered archetypal for acyclic diiminophenol ligands in general, indicating the suitability of complex **2** as a spectroscopic model for **1-Cu**. As is typical for tetranuclear [Cu₄O] diiminophenol complexes (20), no fluorescence was observed from **2** in either the solid or solution states.

By virtue of the predominantly aliphatic character of the external surfaces, the extended supramolecular structure of **2** largely consists of C–H⋯π and other van

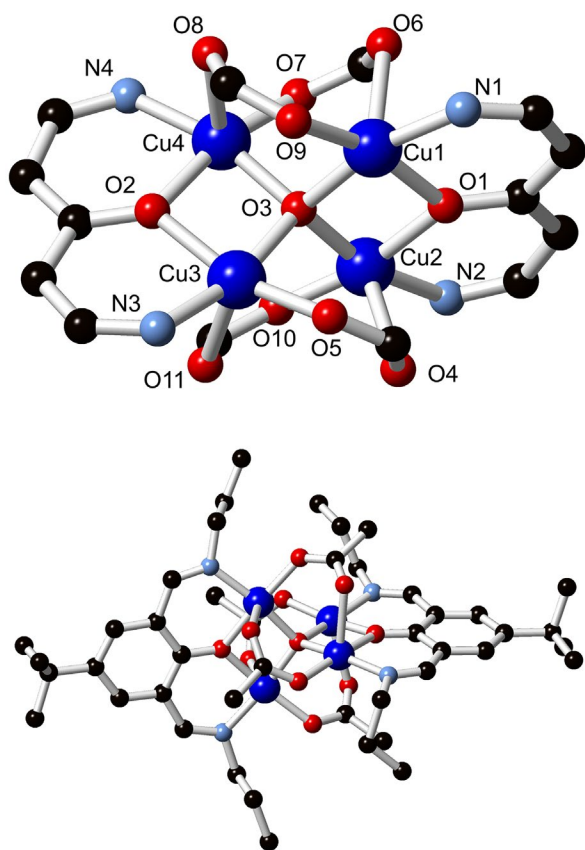


Figure 3. (Colour online) Structure of complex **2**, showing core connectivity with labelling scheme (Top) and structure of the complete complex (Bottom). Hydrogen atoms are omitted for clarity.

der Waals interactions between adjacent complexes. These interactions are best described using a Hirshfeld surface approach (Supporting Information) (21). The most

significant intermolecular interaction, and clearly visible on the related fingerprint plot, are four related C–H···O hydrogen bonding interactions between the imine carbon atoms and coordinating acetato oxygen atoms from adjacent complexes, with the shortest C···O distance 3.411(10) Å between C11 and O8, at a C–H···O angle of 167°. No other significantly directional interactions were clear in the extended structure, although prominent features in the shape index map indicative of C–H··· π interactions involving the propyl chains and the aromatic rings were also evident.

2.1.2. FTIR characterisation of copper binding modes

The FTIR (ATR) spectrum of complex **2** was measured, and compared with the spectra of **1** and **1–Cu** in order to ascertain the nature of the copper binding taking place on the surface of the polymer **1**. In the first instance, a clear distinction can be drawn between the spectrum of the polymer **1** before and after immersion in copper acetate solution. The majority of the organic functional group absorbances are retained between **1** and **1–Cu**, including the overlapping amide C=O and imine C=N stretching bands (maxima 1637 cm⁻¹, with shoulders), and aromatic C–C stretch at 1527 cm⁻¹. After the addition of copper acetate, prominent new absorbances appear at 1585, 1447–1423, 1067, 677 and 619 cm⁻¹, Figure 4. These bands can be assigned to $\nu_{\text{asym}}(\text{COO})$, $\nu_{\text{sym}}(\text{COO}) + \delta_{\text{asym}}(\text{CH}_3)$, $\rho(\text{CH}_3)$, $\delta_{\text{sym}}(\text{COO})$ and $\rho(\text{COO})$, respectively (22), confirming the addition of acetate/acetato species in addition to copper species (which was shown by EDX analysis). Two possibilities were considered for the nature of the Cu/OAc speciation within the polymer **1–Cu**. Firstly, a chelated polymetallic system with bridging acetate ligands of the type seen in complex

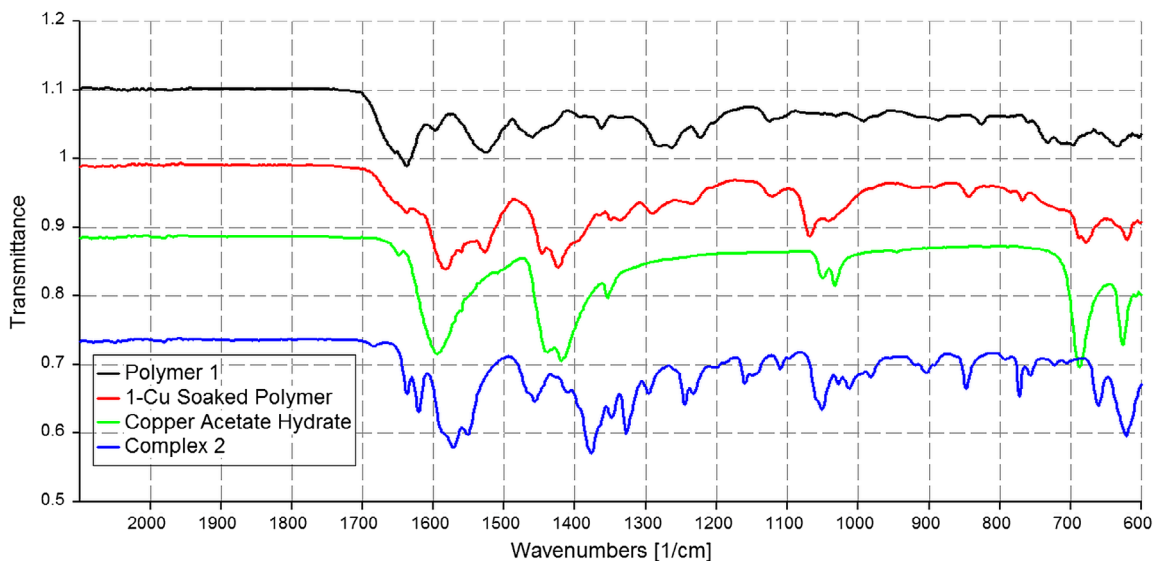
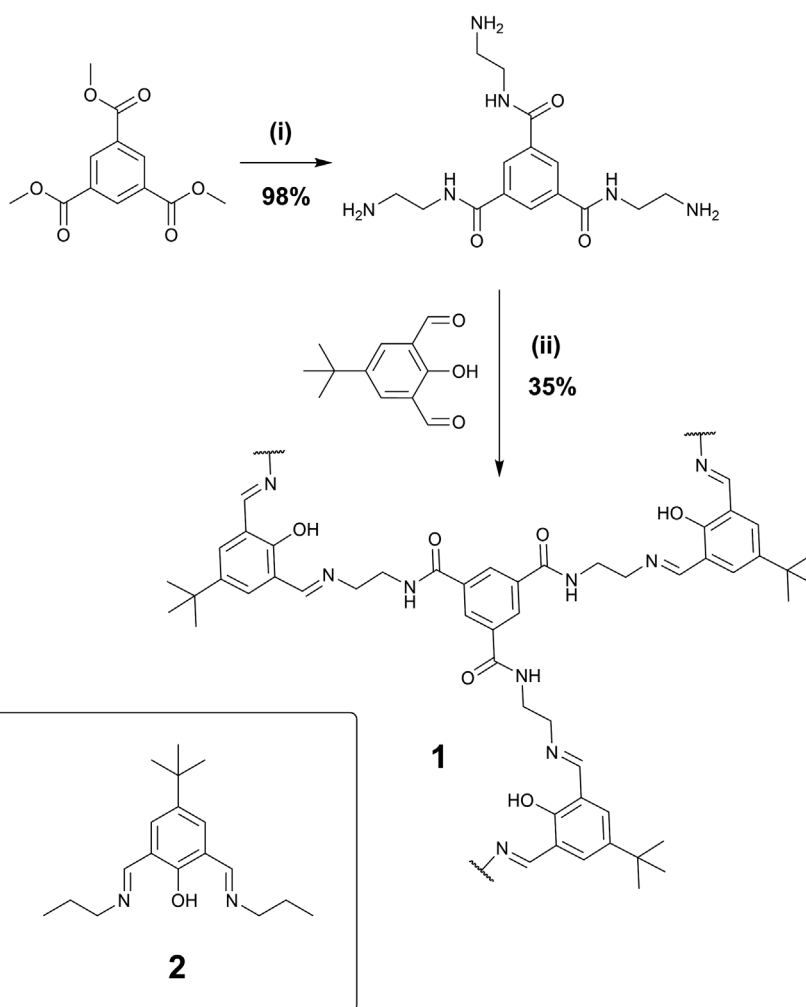


Figure 4. (Colour online) Comparison of the FTIR (ATR) spectra in the range 2100–600 cm⁻¹ of compound **1** (Black, top), **1** after soaking in copper acetate solution (Red, middle upper), pure copper acetate hydrate (Green, middle lower) and model complex **2** (Blue, bottom).



Scheme 1. Synthesis and structure of the polymer **1**, and the structure of model ligand **2**. Reagents and conditions: (i) 1,2-Ethylenediamine, MeOH, RT, 24hr; (ii) EtOH, RT, 18 hr.

2 or related, commonly observed dinuclear species with coordination sphere of the type $[\text{Cu}_2(\text{L})(\text{OAc})_2(\text{X})_2]$ (X = solvent/anion) (**23**) was considered. The lack of measurable fluorescence from **1-Cu** discounts some of the other possible dinuclear complexes of the type $[\text{Cu}_2(\text{L})_2(\text{X})_2]$ (**20**). Secondly, direct adsorption of a symmetrically bridged $[\text{Cu}_2(\text{OAc})_4(\text{X})_2]$ (X = solvent) paddlewheel-type complex on the surface of the polymer can be envisaged, without appreciable coordination within the Schiff-base pocket. To allow for a direct comparison, the FTIR-ATR spectrum of copper acetate hydrate was also collected under the same conditions, Figure 4.

Comparing the various acetate absorbances (Figure 4), it is clear that **1-Cu** bears a strong resemblance in its infrared spectrum to the sum of **1** and pure copper acetate hydrate; the carboxylate ν_{asym} and ν_{sym} bands are in close agreement, leading to a value of Δ , the difference between the two, of $\sim 165 \text{ cm}^{-1}$ for **1-Cu**, *c.f.* the value measured here for copper acetate hydrate of 175 cm^{-1} . This parameter is known to be particularly indicative for the

nature of the carboxylate binding, and takes values ranging from $< 100 \text{ cm}^{-1}$ for chelating carboxylates, $\sim 160 \text{ cm}^{-1}$ for ionic carboxylates and fully symmetric bridging, and can be $> 300 \text{ cm}^{-1}$ for monodentate or unsymmetrically bridging carboxylates (**24**).

In contrast to **1-Cu**, complex **2** exhibits a marked increase in Δ to 200 cm^{-1} , owing to the red-shifted $\nu_{\text{sym}}(\text{COO})$ band observed at 1376 cm^{-1} . This observation suggests a lower symmetry character to the carboxylate bridging mode in **2** compared to copper acetate hydrate and **1-Cu**. This is corroborated by the X-ray crystal structure, in which each of the four unique carboxylate groups coordinates to one axial and one equatorial site of the square pyramidal copper ions; as outlined above, the two Cu–O bond distances for each acetate ligand differ by $0.390(12) \text{ \AA}$ on average, or *ca.* 15–20% of the average Cu–O bond length. Although statistically much less meaningful, this difference is also evident in a greater carbon-oxygen double bond character for the more weakly bound oxygen atom, the bond distances of which fall (on average) $0.06(2)$

Å shorter than those of the more strongly bound oxygen atom, for each of the four ligands. The axial-equatorial bridging of acetato ligands is also commonly observed for the dinuclear complexes of related ligands where square pyramidal coordination geometries are observed (23), as a result of the rigidly coplanar bridging from the chelating diiminophenol group. In comparison to the differences seen in the asymmetric and symmetric COO stretching frequencies, **1-Cu**, **2** and copper acetate hydrate all share relatively similar values for the remaining identifiable absorbances, with only the $\delta_{\text{sym}}(\text{COO})$ absorbance for **2** red-shifted by ca 25 cm⁻¹ for complex **2** compared to **1-Cu** and copper acetate.

The sum of these spectroscopic observations would imply a strong relationship between the structure of the bound copper ions in **1-Cu** to the 'paddlewheel' structure of copper acetate and its solvates, rather than the diiminophenolate-chelated species observed in **2** and related complexes. In combination with the minimal surface area and low adsorption capacity of **1** for copper ions, it is implied that **2** adsorbs copper by acting as a nucleation site for the deposition of copper acetate or a related solvate from solution, rather than by acting as a chemisorbant *per se*.

To further probe the interaction of **1** with *d*-block metal ions, equivalent metal soaking experiments were carried out using methanolic solutions of cobaltous acetate tetrahydrate and zinc acetate dihydrate. In the case of the Co(II) species, essentially equivalent behaviour was observed. Although, unlike the Cu(II) equivalent, the paddlewheel form of Co(II) acetate is not dominant (25), the cobalt-soaked polymer exhibited an infrared spectrum essentially equivalent to the sum of the free polymer and the precursor metal salt. Soaking was accompanied by a darkening in colour of the solid, and similarly to the copper case, loss of the ligand fluorescence signal. On the other hand, exposure of the polymer to Zn(OAc)₂·2H₂O led to broadening and reduction in intensity of the $\nu_{\text{sym}}(\text{COO})$ absorbance and variations in the positions and relative intensities of the CH₃ rocking modes compared to pure zinc acetate dihydrate, indicative of some degree of reaction between the two species. In addition, the fluorescence spectrum of the zinc-soaked **1** exhibited a notable blue-shift, to an emission maximum of 518 nm (cf. 560 nm for the pure polymer, outlined above). This emission behaviour is more consistent with a coordinated diiminophenol moiety, and similar to the emission spectra observed for zinc complexes of related ligands (26). The implication of a more substantial interaction between Zn(II) and polymer **1**, in comparison to the outcome with Cu(II), is in keeping with the chemical properties of the two acetates; the substantially lessened tendency for rigid paddlewheel-type coordination behaviour in the

zinc case (27), and wider range of possible coordination geometries would be expected to favour coordination in this particular instance. Elucidating the exact nature of the interaction between **1** and Zn(II) ions will be the subject of further studies.

3. Conclusions

We have prepared a new organic diiminophenol-based polymer **1** from the reaction between 4-*tert*-butyl-2,6-diformylphenol and an aggregation-inducing tris(2-aminoethyl)-benzene-1,3,5-tricarboxamide derivative. Compound **1**, which exhibits a granular spherical morphology and is amorphous by X-ray powder diffraction, acts as a substrate for the deposition of copper acetate from alcohol solution. Energy-dispersive X-ray spectroscopy and FTIR studies, including comparison with the discrete tetranuclear model compound **2**, implied that the mechanism of adsorption was based on nucleation of a copper acetate or related cupric salt on the surface of the polymer, rather than binding within the Schiff-base compartments of the polymer itself. Adsorption of Co(II) ions yielded similar results, while Zn(II) ions showed some tendency for a chemical transformation on the polymer surface. These results represent a continuation of on-going studies into the interactions between transition metal ions in the solution state and soft-matter host materials, elucidating the precise nature of which remains a crucial challenge in materials chemistry.

4. Experimental

4.1. Materials and methods

All chemicals and HPLC solvents were purchased from Sigma-Aldrich Ireland, Merck or Fisher Scientific and used without further purification unless otherwise stated. Trimethyl benzene-1,3,5-tricarboxylate was prepared from trimesic acid using literature methods (28). NMR data were recorded on a Bruker DPX-400-Avance spectrometer (400.13 (¹H) and 100.6 (¹³C) MHz) and on a Bruker AV-600 spectrometer (600.13 (¹H) and 150.2 (¹³C) MHz) in commercial available deuterated solvents. Chemical Shifts δ are reported in ppm relative to SiMe₄ (= 0 ppm) and are referenced relative to the internal solvents signal, (J in Hz). Data were processed with MestReNova software. Infrared spectra were recorded on Perkin-Elmer-One FT-IR spectrometer equipped with an Attenuated Total Reflectance (ATR) sampler, solid samples were recorded directly as neat samples; in cm⁻¹. Mass spectra were recorded on a Mass Lynx NT V 3.4 on a Waters 600 controller connected to a 996 photodiode array detector with HPLC-grade methanol or acetonitrile as carrier solvents. SEM images were taken using a Carl Zeiss Ultra SEM instrument, using either in-lens

detection or SE2 in the Advanced Microscopy Laboratory, CRANN, Trinity College Dublin. Samples were deposited onto clean silicon wafers with a thick silicon dioxide layer and all samples prepared were covered with an additional Pd/Au conductive layer using a Cressington 208 HR high resolution sputter coater. EDX measurements were carried out using a Carl Zeiss Ultra SEM that was equipped with an Oxford Instruments Inca System EDX setup. The samples used for EDX analysis were uncoated. Thermogravimetric analysis was carried out using a Perkin Elmer Pyris 1 TGA, with samples mounted in alumina crucibles and heated under a nitrogen purge flow of 20 mL/min at heating rates of 5 °C/min. Gas adsorption isotherms were measured using a Quantachrome Autosorb IQ gas sorption analyser. Chemically pure (CP, N4.5) grade He and CO₂ gases from BOC gases were used for the measurements. The sample was de-gassed under dynamic vacuum at 50 °C for 24 h prior to the measurements. Fluorescence spectra were measured on a Varian Cary Eclipse fluorimeter with excitation and emission slits fixed at 2.5 nm for all measurements. X-ray powder diffraction data were collected using a Bruker D2 Phaser instrument using Cu K α ($\lambda = 1.5418 \text{ \AA}$) radiation in Bragg-Brentano geometry, with samples mounted on a zero-background silicon single crystal sample holder. Patterns were collected in the 2θ range 5–55° in 0.01° increments.

4.2. X-ray crystallography

Diffraction data were collected using a Bruker APEX-II Duo dual-source instrument using Mo K α ($\lambda = 0.71073 \text{ \AA}$) radiation. The data were collected using ω and φ scans with the crystal immersed in oil and maintained at a constant temperature of 100 K using a Cobra cryostream. The data were reduced and processed using the Bruker APEX suite of programs (29). A multi-scan absorption correction was applied using SADABS (30). The diffraction data for **2** were solved using SHELXT and refined by full-matrix least squares procedures using SHELXL-2015 within the OLEX-2 GUI (31–33). The functions minimized were $\sum w(F_o^2 - F_c^2)$, with $w = [\sigma^2(F_o^2) + aP^2 + bP]^{-1}$, where $P = [\max(F_o^2) + 2F_c^2]/3$. Non-hydrogen atoms were refined with anisotropic displacement parameters. All hydrogen atoms were placed in calculated positions and refined with a riding model, with isotropic displacement parameters equal to either 1.2 or 1.5 times the isotropic equivalent of their carrier atoms as appropriate. Specific refinement strategies are outlined in the crystallographic information file (cif).

Crystal data for **2**: C₄₄H₆₆Cu₄N₄O₁₁ ($M = 1081.16 \text{ g/mol}$): monoclinic, space group $P2_1/c$ (No. 14), $a = 12.4474(7) \text{ \AA}$, $b = 26.4033(15) \text{ \AA}$, $c = 15.8247(9) \text{ \AA}$, $\beta = 110.345(2)^\circ$, $V = 4876.4(5) \text{ \AA}^3$, $Z = 4$, $T = 100.0 \text{ K}$, $\mu(\text{Mo K}\alpha) = 1.780 \text{ mm}^{-1}$, $D_{\text{calc}} = 1.473 \text{ g/cm}^3$, 49,627

reflections measured ($3.084^\circ \leq 2\theta \leq 50.998^\circ$), 9036 unique ($R_{\text{int}} = 0.0676$, $R_\sigma = 0.0589$) which were used in all calculations. The final R_1 was 0.0713 ($I > 2\sigma(I)$) and wR_2 was 0.2084 (all data). CCDC 1540122.

4.3. Ligand synthesis

4.3.1. *N,N',N''-tris(2-aminoethyl)benzene-1,3,5-tricarboxamide*

The title compound was prepared by a method similar to that reported by Xu et al. (17) Under an argon atmosphere, ethylenediamine (20 mL) was added to a flask. Trimethyl benzene-1,3,5-tricarboxylate (0.51 g, 2.02 mmol) was dissolved in methanol (20 mL) and added dropwise to the solution of ethylenediamine (EDA) under an argon atmosphere at 0 °C. The solution was stirred at 0 °C for 30 min and then at room temperature for 24 h. The excess ethylenediamine was removed *in vacuo*, and the residue was dissolved in a mixture of toluene/methanol (10:1) and the solvent was again removed under vacuum to remove the residual ethylenediamine. This process was repeated three times and the product was obtained as a sticky yellow solid. Yield: 0.67 g (98%); δ_{H} (400 MHz, DMSO- d_6) $\delta = 8.61$ (t, $J = 5.6 \text{ Hz}$, 3H, H⁴), 8.39 (s, 3H, H⁵), 3.29 (q, $J = 6.2 \text{ Hz}$, overlapping with water peak, H³), 2.70 (t, $J = 6.5 \text{ Hz}$, 6H, H²); δ_{C} (101 MHz, DMSO- d_6) $\delta = 165.7, 135.1, 128.4, 43.2, 41.3$; m/z (ESI⁺) 337.1989 ([M + H]⁺, calculated for C₁₅H₂₅N₆O₃⁺ 337.1983; ν_{max} (ATR, cm⁻¹) 3278m, 3064m, 2932m, 2870m, 1639 s, 1589m, 1534s, 1430m, 1387m, 1287s, 1186m, 1108m, 1071m, 1035m, 913m, 852m, 821m, 703s.

4.3.2. Polymer 1

4-*tert*-Butyl-2,6-diformylphenol (37 mg, 178 μmol) was dissolved in EtOH (5 mL). *N,N',N''-tris(2-aminoethyl)benzene-1,3,5-tricarboxamide* (40 mg, 119 μmol , 0.66 eq.) was dissolved in ethanol (2 mL) before being added to the solution of 4-*tert*-Butyl-2,6-diformylphenol in ethanol. A yellow precipitate immediately formed and the mixture was stirred at room temperature for 18 h. The solution was filtered and the precipitate was washed with ethanol before drying *in vacuo*, with the product obtained as a yellow solid. Yield: 27 mg (35%); m.p. > 300 °C; Found C, 61.39; H, 6.40; N, 12.60; Calculated for C₆₆H₇₈N₁₂O₉·6H₂O C, 61.38; H, 7.02; N, 13.01; δ_{C} {SS-CP-MAS} (101 MHz) $\delta = 167.2, 141.5, 136.3, 132.5, 131.0, 118.8, 60.8, 41.6, 34.1, 31.6$; ν_{max} (ATR, cm⁻¹) 3287w br, 2957m, 2865w, 1637s sh, 1597w, 1527s sh, 1459m sh, 1363m, 1265m sh, 1223m, 1124w, 992w, 825w, 733m, 696m, 633m.

4.3.3. Complex 2

4-*tert*-Butyl-2,6-diformylphenol (100 mg, 485 μmol) and *n*-propylamine (80 μL , 970 μmol , 2 eq.) were combined in 10 mL of methanol, and the mixture was heated at

reflux for one hour. On cooling, the solvent was removed *in vacuo*, and the yellow oily residue was redissolved in 10 mL of acetonitrile. A 2 mL portion of this solution was combined with a solution of copper(II) acetate hydrate (38 mg, 190 μmol , 2 eq) in 4 mL of acetonitrile, and the resulting green solution was sealed and left to stand at room temperature for 48 h. Dark green crystals of the product **2** were isolated by filtration, washed with acetonitrile and dried in air. Yield 9.8 mg (9% overall). Phase purity was determined by X-ray powder diffraction (Supporting Information). m.p. 274–276 °C (decomp); Found C, 48.24; H, 6.13; N, 5.02; Calculated for $\text{C}_{44}\text{H}_{66}\text{N}_4\text{O}_{11}\text{Cu}_4$ C, 48.88; H, 6.15; N, 5.18%; ν_{max} (ATR, cm^{-1}) 2964m, 2872w, 1685w, 1638m, 1622m, 1572s sh, 1456m sh, 1376s sh, 1348m, 1328s, 1295m, 1244m, 1158w, 1109 w, 1051s, 1012w, 982w, 903w, 846m, 771m, 756w, 660m, 619s.

Acknowledgements

We thank Dr Manuel Reuther (TCD) for assistance with SS-NMR.

Disclosure statement

No potential conflict of interest was reported by the authors.

Funding

This work was supported by the Irish Research Council (IRC) for a Postdoctoral Fellowship [grant number GOIPD/2015/446 to CSH]; the Science Foundation Ireland (SFI) for SFI PI Awards [grant number 13/IA/1865 to TG], [grant number 13/IA/1896 to WS], TCD Dean of Research Pathfinder Award (TG and CSH); the European Research Council [grant number ERC/CoG 2014 – 647719 to WS], the Erasmus Programme (travel grant to MKH) and TCD School of Chemistry for financial support.

References

- (1) (a) Canrinus, T.R.; Cerpentier, F.J.R.; Feringa, B.L.; Browne, W.R. *Chem. Commun.* **2017**, 53, 1719–1722; (b) Gunnlaugsson, T. *Nat. Chem.* **2016**, 8, 6–7; (c) Tong, K.W.K.; Dehn, S.; Webb, J.E.A.; Nakamura, K.; Braet, F.; Thordarson, P. *Langmuir* **2009**, 25, 8586–8592.
- (2) (a) dos Santos, C.M.G.; Boyle, E.M.; De Solis, S.; Kruger, P.E.; Gunnlaugsson, T. *Chem. Commun.* **2011**, 47, 12176–12178; (b) Kotova, O.; Daly, R., dos Santos, C.M.G., Boese, M., Kruger, P.E., Boland, J.J., Gunnlaugsson, T. *Angew. Chem. Int. Ed.* **2012**, 51, 7208–7212; (c) Pandurangan, K.; Kitchen, J.A.; Blasco, S.; Boyle, E.M.; Fitzpatrick, B.; Feeney, M.; Kruger, P.E.; Gunnlaugsson, T. *Angew. Chem. Int. Ed.* **2015**, 54, 4566–4570; (d) Hawes, C.S.; Byrne, K.; Schmitt, W.; Gunnlaugsson, T. *Inorg. Chem.* **2016**, 55, 11570–11582; (e) de Silva, A.P.; Gunaratne, H.Q.N.; Gunnlaugsson, T.; McCoy, C.P.; Maxwell, P.R.S.; Rademacher, J.T.; Rice, T.E. *Pure & Appl. Chem.* **1996**, 68, 1443–1448; (f) Gunnlaugsson, T.; Bichell, B.; Nolan, C. *Tetrahedron Lett.* **2002**, 43, 4989–4992; (g) Duke, R.M.; O'Brien, J.E.; McCabe, T.; Gunnlaugsson, T. *Org. Biomol. Chem.* **2008**, 6, 4089–4092.
- (3) (a) Howe, E.J.; Okesola, B.O.; Smith, D.K. *Chem. Commun.* **2015**, 51, 7451–7454; (b) Foster, J.A.; Piepenbrock, M.-O.M.; Lloyd, G.O.; Clarke, N.; Howard, J.A.K.; Steed, J.W. *Nat. Chem.* **2010**, 2, 1037–1043; (c) Neumann, L.N.; Baker, M.B.; Leenders, C.M.A.; Voets, I.K.; Lafleur, R.P.M.; Palmans, A.R.A.; Meijer, E.W. *Org. Biomol. Chem.* **2015**, 13, 7711–7719.
- (4) (a) Lynes, A.D.; Hawes, C.S.; Ward, E.N.; Haffner, B.; Mobius, M.E.; Byrne, K.; Schmitt, W.; Pal, R.; Gunnlaugsson, T. *CrystEngComm* **2017**, 19, 1427–1438; (b) Kotova, O.; Daly, R.; dos Santos, C.M.G.; Kruger, P.E.; Boland, J.J.; Gunnlaugsson, T. *Inorg. Chem.* **2015**, 54, 7735–7774; (c) Daly, R.; Kotova, O.; Boese, M.; Gunnlaugsson, T.; Boland, J.J. *ACS Nano* **2013**, 7, 4838–4845.
- (5) (a) Cantekin, S.; de Greef, T.F.A.; Palmans, A.R.A. *Chem. Soc. Rev.* **2012**, 41, 6125–6137; (b) Stals, P.J.M.; Everts, J.C., de Bruijn, R., Filot, I.A.W., Smulders, M.M.J., Martín-Rapún, R., Pidko, E.A., de Greef, T.F.A., Palmans, A.R.A., Meijer, E.W. *Chem. Eur. J.* **2010**, 16, 810–821; (c) Desmarchelier, A.; Raynal, M.; Brocorens, P.; Vanthuyne, N.; Bouteiller, L. *Chem. Commun.* **2015**, 51, 7397–7400.
- (6) Desmarchelier, A.; Alvarenga, B.G.; Caumes, X.; Dubreucq, L.; Troufflard, C.; Tessier, M.; Vanthuyne, N.; Ide, J.; Maistriaux, T.; Beljonne, D.; Brocorens, P.; Lazzaroni, R.; Raynal, M.; Bouteiller, L. *Soft Matter* **2016**, 12, 7824–7838.
- (7) (a) Paikar, A.; Pramanik, A.; Haldar, D. *RSC Adv.* **2015**, 5, 31845–31851; (b) Howe, R.C.T.; Smalley, A.P.; Guttenplan, A.P.M.; Doggett, M.W.R.; Eddleston, M.D.; Tan, J.C.; Lloyd, G.O. *Chem. Commun.* **2013**, 49, 4268–4270; (c) Lightfoot, M.P.; Mair, F.S.; Pritchard, R.G.; Warren, J.E. *Chem. Commun.* **1999**, 1945–1946; (d) Rajput, L.; Chernyshev, V.V.; Biradha, K. *Chem. Commun.* **2010**, 46, 6530–6532.
- (8) Banerjee, S.; Adarsh, N.N.; Dastidar, P. *Soft Matter* **2012**, 8, 7623–7629.
- (9) (a) McConnell, A.J.; Wood, C.S.; Neelakandan, P.P.; Nitschke, J.R. *Chem. Rev.* **2015**, 115, 7729–7793; (b) Vardhan, H.; Mehta, A.; Nath, I.; Verpoort, F. *RSC Adv.* **2015**, 5, 67011–67030.
- (10) (a) Bilbeisi, R.A.; Ronson, T.K.; Nitschke, J.R. *Angew. Chem. Int. Ed.* **2013**, 52, 9027–9030; (b) Faulkner, A.D.; Kaner, R.A.; Abdallah, Q.M.A.; Clarkson, G.; Fox, D.J.; Gurnani, P.; Howson, S.E.; Phillips, R.M.; Roper, D.I.; Simpson, D.H.; Scott, P. *Nat. Chem.* **2014**, 6, 797–803; (c) Pelleteret, D.; Clérac, R.; Mathonière, C.; Harté, E.; Schmitt, W.; Kruger, P.E. *Chem. Commun.* **2009**, 45, 221–223; (d) Ferguson, A.; Squire, M.A.; Siretanu, D.; Mitcov, D.; Mathonière, C.; Clérac, R.; Kruger, P.E. *Chem. Commun.* **2013**, 49, 1597–1599.
- (11) (a) Herrmann, A. *Org. Biomol. Chem.* **2009**, 7, 3195–3204; (b) Guiseppone, N.; Lehn, J.-M. *Chem. Eur. J.* **2006**, 12, 1715–1722.
- (12) (a) Pandey, P.; Katsoulidis, A.P.; Eryazici, I.; Wu, Y.; Kanatzidis, M.G.; Nguyen, S.T. *Chem. Mater.* **2010**, 22, 4974–4979; (b) Kandambeth, S.; Mallick, A.; Lukose, B.; Mane, M.V.; Heine, T.; Banerjee, R. *J. Am. Chem. Soc.* **2012**, 134, 19525–19527; (c) Schwab, M.G.; Fassbender, B.; Spiess, H.W.; Thomas, A.; Feng, X.; Müllen, K. *J. Am. Chem. Soc.* **2009**, 131, 7216–7217.
- (13) (a) Pilkington, N.H.; Robson, R. *Aust. J. Chem.* **1970**, 23, 2225–2236; (b) Hoskins, B.F.; Robson, R.; Vince, D. *Chem. Commun.* **1973**, 392–393; (c) Hoskins, B.F.; Robson, R.; Williams, G.A. *Inorg. Chim. Acta.* **1976**, 16, 121–133; (d) Lindoy, L.F. *Supramol. Chem.* **2012**, 24, 448–461.
- (14) (a) Adams, H.; Bailey, N.A.; Bertrand, P.; Rodriguez de Barbarin, C.O.; Fenton, D.E.; Gou, S. *J. Chem. Soc., Dalton*

- Trans.* **1995**, 275–279; (b) Huang, W.; Zhu, H.-B.; Gou, S.-H. *Coord. Chem. Rev.* **2006**, 250, 414–423.
- (15) (a) Jana, A.; Aliaga-Alcalde, N.; Ruiz, E.; Mohanta, S. *Inorg. Chem.* **2013**, 52, 7732–7746; (b) Andruh, M. *Chem. Commun.* **2011**, 47, 3025–3042.
- (16) Chandra, D.; Dutta, A.; Bhaumik, A. *Eur. J. Inorg. Chem.* **2009**, 4062–4068.
- (17) Xu, F.; Xu, J.-W.; Zhang, B.-X.; Luo, Y.-L. *AIChE Journal* **2015**, 61, 35–45.
- (18) (a) Sarkar, M.; Clérac, R.; Mathonière, C.; Hearn, N.G.R.; Bertolasi, V.; Ray, D. *Inorg. Chem.* **2011**, 50, 3922–3933; (b) Wang, X.; Zhao, K.-Q.; Elsegood, M.R.J.; Prior, T.J.; Liu, X.; Wu, L.; Sanz, S.; Brechin, E.K.; Redshaw, C. *RSC Adv* **2015**, 5, 57414–57424.
- (19) (a) Shakya, R.; Keyes, P.H.; Heeg, M.J.; Moussawei, A.; Heiney, P.A.; Verani, C.N. *Inorg. Chem.* **2006**, 45, 7587–7589; (b) Ghosh, A.K.; Ray, D. *Polyhedron* **2013**, 52, 370–376; (c) Roy, P.; Nandi, M.; Manassero, M.; Riccò, M.; Mazzani, M.; Bhaumik, A.; Banerjee, P. *Dalton Trans.* **2009**, 9543–9554.
- (20) Das, S.; Jana, S.; Chakraborty, P.; Sanyal, R.; Maiti, D.K.; Guchhait, N.; Zangrando, E.; Das, D. *Eur. J. Inorg. Chem.* **2014**, 5432–5442.
- (21) (a) Spackman, M.A.; Jayatilaka, D. *CrystEngComm* **2009**, 11, 19–32; (b) McKinnon, J.J.; Jayatilaka, D.; Spackman, M.A. *Chem. Commun.* **2007**, 3814–3816.
- (22) Mathey, Y.; Greig, D.R.; Shriver, D.F. *Inorg. Chem.* **1982**, 21, 3409–3413.
- (23) (a) Sarkar, S.; Majumder, S.; Sasmal, S.; Carrella, L.; Rentschler, E.; Mohanta, S. *Polyhedron* **2013**, 50, 270–282; (b) Arbaoui, A.; Redshaw, C.; Sanchez-Ballester, N.M.; Elsegood, M.R.J.; Hughes, D.L. *Inorg. Chim. Acta* **2011**, 365, 96–102; (c) Anekwe, J.; Hammerschmidt, A.; Rompel, A.; Krebs, B. *Z. Anorg. Allg. Chem.* **2006**, 632, 1057–1066; (d) Kitchen, J.A.; Martinho, P.N.; Morgan, G.G.; Gunnlaugsson, T. *Dalton Trans.* **2014**, 43, 6468–6479.
- (24) Deacon, G.B.; Phillips, R.J. *Coord. Chem. Rev.* **1980**, 33, 227–250.
- (25) van Niekerk, J.N.; Schoening, F.R.L. *Acta Crystallogr.* **1953**, 6, 609–612.
- (26) Chakraborty, P.; Adhikary, J.; Samanta, S.; Majumder, I.; Massera, C.; Escudero, D.; Ghosh, S.; Bauza, A.; Frontera, A.; Das, D. *Dalton Trans.* **2015**, 44, 20032–20044.
- (27) Bureekaew, S.; Amirjalayer, S.; Schmid, R. *J. Mater. Chem.* **2012**, 22, 10249–10254.
- (28) Li, Z.; Feng, X.; Zou, Y.; Zhang, Y.; Xia, H.; Liu, X.; Mu, Y. *Chem. Commun.* **2014**, 50, 13825–13828.
- (29) Bruker APEX-3, Bruker-AXS Inc.: Madison, WI, 2016.
- (30) SADABS, Bruker-AXS Inc.: Madison, WI, 2016.
- (31) Sheldrick, G.M. *Acta Crystallogr. Sect. A* **2015**, 71, 3–8.
- (32) Sheldrick, G.M. *Acta Crystallogr. Sect. C* **2015**, 71, 3–8.
- (33) Dolomanov, O.V.; Bourhis, L.J.; Gildea, R.J.; Howard, J.A.K.; Puschmann, H. *J. Appl. Cryst.* **2009**, 42, 339–341.